Check for updates

The changing relationship between the convection over the western Tibetan Plateau and the sea surface temperature in the northern Bay of Bengal

By B. H. VAID* and X. SAN LIANG, *School of Marine Sciences, Nanjing University of Information Science and Technology (NUIST), Nanjing, China*

ABSTRACT

Using the National Oceanic and Atmospheric Administration (NOAA) sea surface temperature (SST) data, we found that the peak Indian summer monsoon season SST in the northern Bay of Bengal (NBOB) has been increased since late 1990s. Moreover, the NBOB SST reveals an increasing trend after 1999 (hereafter POST99), whereas prior to 1999 (PRE99) the trend is decreasing. During POST99, the NBOB SST facilitates a deep convection, while during PRE99 it does not seem so. A robust causality analysis also reveals a large impact on the convection and precipitation over the western Tibetan Plateau during POST99, whereas no significant causality is identified before 1999. Besides, regressions onto the NBOB SST result in a cyclonic circulation pattern and ascending winds on upper vertical levels over the western Tibetan Plateau during POST99, which are distinctly different from those during PRE99.

Keywords: Bay of Bengal, sea surface temperature, Tibetan Plateau

1. Introduction

The Bay of Bengal (BOB) is a northern extension of the Indian Ocean, located between India and Sri Lanka in the west, Bangladesh to the north and Myanmar (Burma) and the northern part of the Malay Peninsula to the east. It is known as the one of the most important heat source regions of the tropical oceans during the months of July and August (Webster, 1995; Rao et al., 2002), and these two months are considered to be the principal monsoon months in India, accounting for nearly 75% of the annual rainfall over a major part of the country (Raghavan, 1973; Gadgil et al., 2005; Rajeevan et al., 2010). The BOB region is observed to have some prevalent characteristics [for example, the presence of large freshwater input, lowest surface salinities, high sea surface temperature (SST), variable monsoonal forcing, excess evaporation over precipitation (~2 m/year), fresh water influx from adjoining rivers (1.625×10^{12} m³/year), etc.], making it one of the important tropical oceans in the world (Hacker et al., 1998; Shenoi et al., 2002; Roxy and Tanimoto, 2007). The BOB is rarely studied in terms of variabilities on climate scales, although the seasonal variability in hydrography and circulation is well documented (e.g. McCreary et al., 1993; Schott and McCreary, 2001; Shankar et al., 2002; and references therein). It is of huge scientific interest due to its role in the seasonal monsoon rainfall over the surrounding land (Bruce, 1968;

Alam et al., 2003; Yuan and Han, 2006; Oliver and Thompson, 2010; Girishkumar and Ravichandran, 2012, Girishkumar et al., 2013; Polanski et al., 2013). For example, it impacts Indian subcontinent rainfall through a seasonal monsoon trough that extends from north-west India to the head BOB region (Polanski et al., 2013), influences the monsoon rainfall in Bangladesh (Salahuddin et al., 2006) and modifies the precipitation over the southern China region (Yangtze River Valley in particular) with moisture flux that converges and turns north-eastwards in the vicinity of the Tibetan Plateau (TP) (Xu et al., 2008b). Besides, it is also observed to be associated with the TP rainfall through a south Asian monsoon-related moisture corridor that extends from the BOB along the Brahmaputra River (Wu and Zhang, 1998; Chen et al., 2012; Yang et al., 2014). However, the BOB SST is rarely studied in terms of its explicit connection with the precipitation over the TP. This is not what one would expect, considering the importance of the TP, which has been referred to as 'the world's water tower' in the Asia; its precipitation variability is closely related to the regional glaciers, river discharge, plant phenology and natural hazards (Xu et al., 2008a; Yao et al., 2012; Dorji et al., 2013; Molg et al., 2014), affecting the climate and socioeconomic conditions throughout many parts of Asia (Xu et al., 2008b; Ma et al., 2017).

In the present study, we use the long term SST observational product (Reynolds et al., 2007; Casey et al., 2010) to investigate

---

*Corresponding author. e-mail: bakshi32@gmail.com, vaidbh@hotmail.com
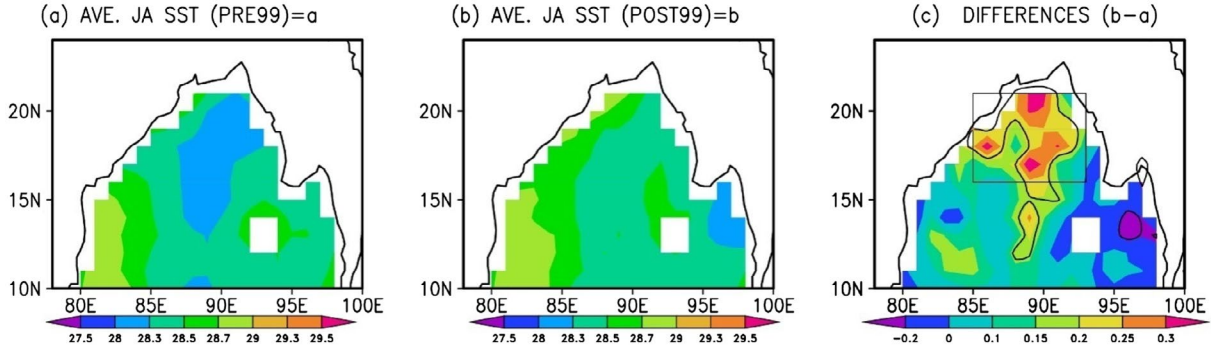
1

Fig. 1. BOB SST (in °C) averaged over JA for (a) PRE99 (b) POST99. (c) The difference between (a) and (b). The regions enclosed in black contours are significantly different from zero at a 99% confidence level.
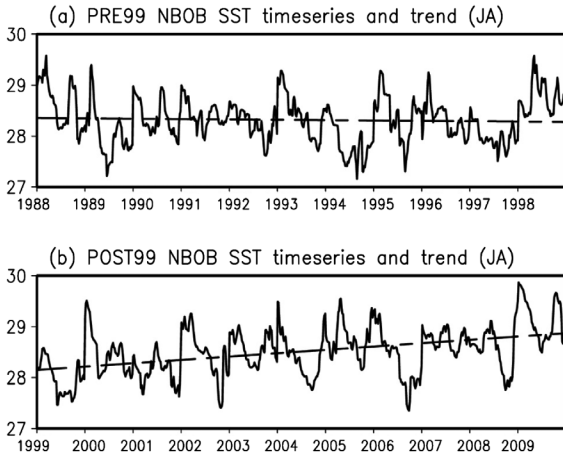

Fig. 2. (a) Time series plot (solid lines) and linear trend (dashed line) of the NBOB SST (in °C) during JA of PRE99 (daily data from 1988 to 1998) (b) Time series (solid lines) and linear trend (dashed line) of the NBOB SST during JA of POST99 (daily data from 1999 to 2009). The linear trends are statistically significant at a 99% confidence level.

the BOB SST variability and its relationship with the western TP during the peak summer monsoon seasons of 1988–2009. We first list the data source, then give a brief presentation of the results. This study is summarised in Section 4.

2.   Data

The data-sets used in this study include the following: (1) National Centre for Environmental Prediction (NCEP) – DOE AMIP 2 reanalysis daily data sets for horizontal and meridional wind fields, geopotential height, air temperature and relative humidity (Kanamitsu et. al., 2002), provided by the NOAA/OAR/ESRL PSD, Boulder, Colorado, USA (http://www.esrl.noaa.gov/psd/); (2) Asian Precipitation – Highly-Resolved Observational Data Integration Towards Evaluation (APHRODITE's) of Water Resources for precipitation (http://www.chikyu.ac.jp/precip/english/products.html); (Yatagai et. al., 2012); (3) the National Oceanic and Atmospheric Administration (NOAA)

1/4° daily Optimum Interpolation SST version 2 (http://www.ssmi.com/amsr/amsr_browse.html); (4) NOAA Interpolated OLR team product (http://www.esrl.noaa.gov/psd/) for outgoing long-wave radiation (OLR).

3.   Results

The daily NOAA SST data is used to investigate the climate variability in the SST over the BOB during the peak monsoon season of India. We particularly focus on two periods: the period 1988–98 (PRE99) and the period 1999–2009 (POST99). The periods PRE99 and POST99 are chosen because the first leading empirical orthogonal function (EOF) mode of the POST99 tropical Pacific sea surface temperature anomalies (SSTA) has shown maximum warming in the central Pacific (around 150°W), whereas the PRE99 EOF1 mode shows a warming in the eastern Pacific (Xiang et. al., 2013; Chung and Li, 2013; Vaid and Liang, 2015). Besides, it is well known that El Niño facilitates the SST variations in the BOB during July and August (Singh et al., 2001), we hence focus on the peak monsoon time July and August. Figure 1 shows (a) the JA averaged SST for the period PRE99, (b) same SST but for the period POST99 and (c) the difference between the above two (POST99 minus PRE99). Clearly, the mean JA SSTs for both PRE99 and POST99 are above 28 °C (Figs. 1a and b) in most of the northern part of the bay, which is conducive to enhanced convective precipitation. [Recall that, to sustain such convection, SST has to exceed a critical threshold of about 28 °C (Gadgil et al., 1984; Graham and Barnett, 1987; Lau et al., 1997)]. We see a substantial difference between the PRE99 and POST99 SSTs in the north BOB region: Long. = 85°E–93°E, Lat = 15°N – 21°N [northern BOB (NBOB) region; marked with rectangle in the Fig. 1]. Further analysis shows that the NBOB SST increases substantially after 90s (Fig. 1). The change is mostly significant at the 99% level based on the student's t test; the significant region is marked with black contours in Fig. 1c. The time series of the NBOB SST is plotted in Fig. 2, respectively, for PRE99 (maximum: 29.6, minimum: 27.1, mean: 28.3, standard devia-
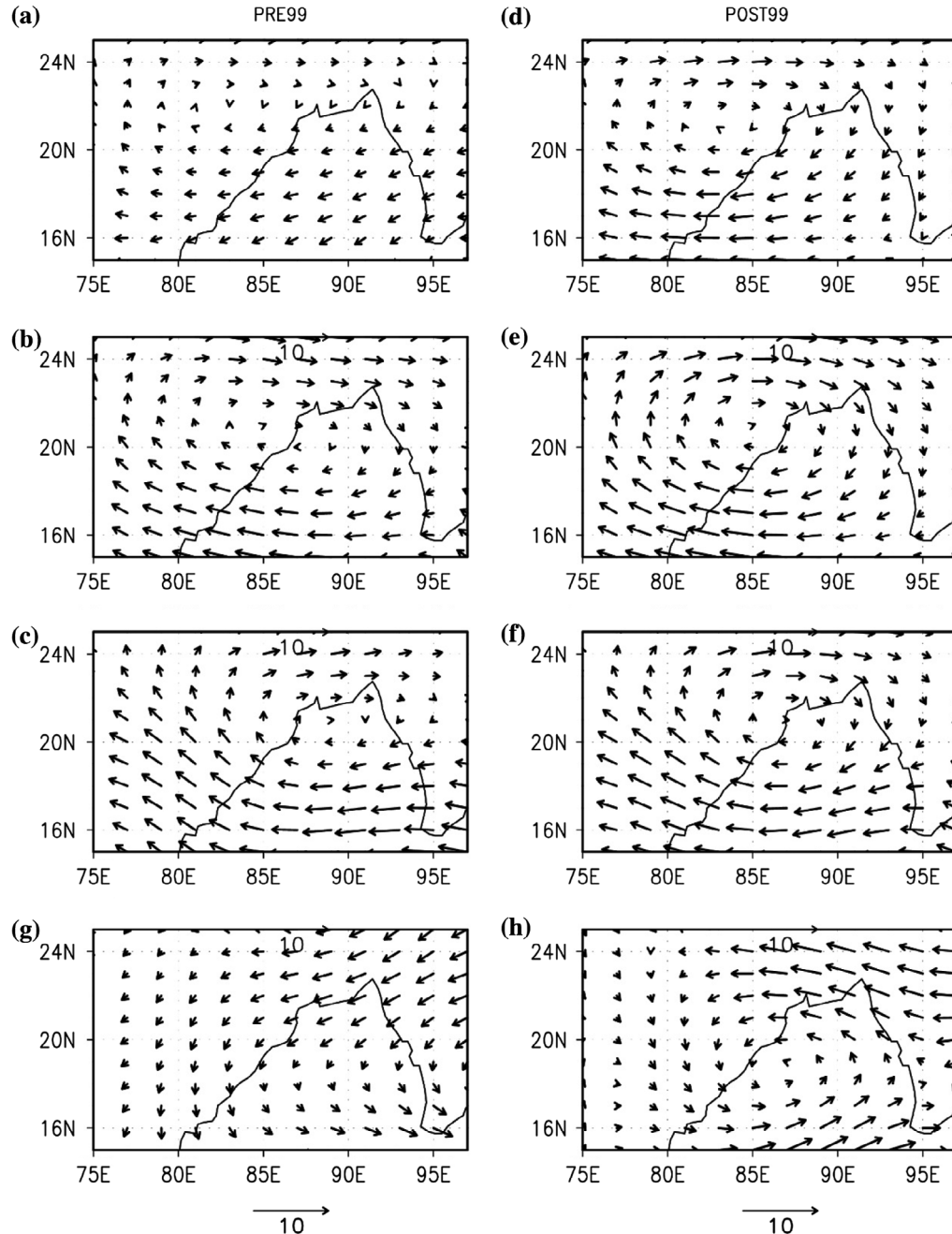
Fig. 3. (a)–(f) Wind vector (in m/s) at 400mb, 500mb and 850mb regressed onto the JA NBOB SST daily series for PRE99 (left panel) and POST99 (right panel). Regression coefficient is statistically significant at a 99% level. (g) and (h) are the vertical differences of the regressed wind vectors (200 mb wind minus 850 mb wind) for PRE99 and POST99, respectively. Shown are regressed wind vectors on a 1°×1° latitude–longitude grid.

tion: 0.4, variance: 0.2) and POST99 (maximum: 29.9, minimum: 27.3, mean: 28.5, standard deviation: 0.5, variance: 0.3). Clearly, we see that during POST99 the NBOB SST is significantly increased in comparison to PRE99.

Figure 2 also shows, respectively, the linear trends of the NBOB SST for the two periods (Figs. 2a and b). A clearly decreasing trend is seen before 1999, whereas after 1999 an

increasing trend is identified. Obviously the NBOB SST is experiencing a climatic change around 1999. First, during PRE99, the SST change is mild (0.075 °C), but during POST99 it experiences a large change (0.7 °C). While a rise of 0.075 °C might be within the measurable error since the global SST is observed to go up at a rate of 0.06 °C per decade from 1970 to1999 (Xue et al., 2013), the warming during POST99 is really remarkable.
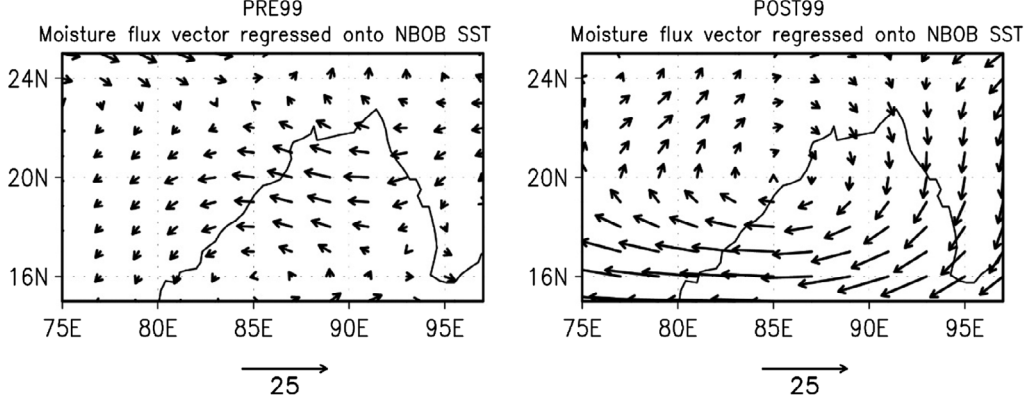
Fig. 4. Moisture flux vector (in kg/m/s) regressed onto the JA NBOB SST for PRE99 (left panel) and POST99 (right panel). The regression coefficient is statistically significant at a 99% level. Shown are the regressed moisture flux vectors on a $1° \times 1°$ latitude–longitude grid.

These completely different trends are statistically significant. At a 99% confidence level, the values of the two slopes are, respectively, [−1.1 ± 2.2] and [10.0 ± 2.4] (both to be multiplied by 10E-4). That is to say, they lie within: [−3.3, 1.1] and [7.6, 12.4] which clearly do not have overlap at all.

The NBOB is one of the important regions of deep convection associated with the Indian summer monsoon because of its capability of absorbing heat from and transferring heat to surrounding lands. In order to see how deep the convection is over the BOB during the different epochs, we regress the wind vector at 400mb, 500mb and 850mb onto the NBOB SST series for both PRE99 and POST99 (Fig. 3a–f) using the least square regression method. The regression equation has the form Y = a + bX, where X and Y are two variables, *b* is the slope of the line and *a* is the y-intercept. In this case, X is the NBOB SST time series and Y the series of gridded wind vector values on a $1° \times 1°$ latitude–longitude grid (see Fig. 3). Both the series have a time resolution of 1 day, and the regressed wind vectors are plotted in Fig. 3. It is well known that the basic element which drives the convection is the vertical variations of wind over a specific region (e.g. Anber et al., 2014). We hence also plot the vertical wind shears (200 mb minus 850 mb level). As shown in Fig. 3g,h, except for the cyclonic pattern, which is consistent with the convection, the difference in the shear during the two epochs is clearly seen—the convection has been significantly strengthened recently. More specifically, the NBOB SST seems to induce the wind circulation up to 400mb level during POST99, while during PRE99 it does not. That is to say, the NBOB SST facilitates a deeper convection after 1999.

To see more about this, we compute the total horizontal mean flux components (zonal and meridional) of water vapour:

$$Q'_\lambda = \frac{1}{g} \int_{p_u}^{p_s} q' u \, dp$$

$$Q'_\emptyset = \frac{1}{g} \int_{p_u}^{p_s} q' v \, dp$$

where Q'_λ is the zonal component and $Q'_\emptyset$ is the meridional component of the vertically integrated total mean vapour flux and q is the specific humidity. The constant g is the gravitational acceleration; it is divided by to ensure a unit of kg s^{-1} m^{-1}. The top layer of the vertical integration considered here is 300 hPa because above this level the water vapour content is negligible (Kalnay et al., 1996). The fluxes regressed onto the NBOB SST for PRE99 and POST99 are shown in Fig. 4. Clearly, the NBOB SST facilitates a shallower convection over the BOB during PRE99.

The distinct vertical variations of winds and moisture flux vector (Figs. 3 and 4) will have different impacts on the monsoon precipitation over the surrounding regions. To see this, a newly developed causality analysis technique based on the Liang-Kleeman information flow theory is used. This technique is capable of quantitatively evaluating the drive and the feedback causal relation between any pair of time series, whether their dynamics are foreknown or not. It can be used to address the importance of different forcing components in a climate system in a quantitative but a model independent way. This analysis uses information flow to quantify the causality between time series. Suppose we have two series X_1 and X_2, then, as proved in Liang (2014) and Liang (2016), the rate of information flowing from the latter to the former, $T_{2 \to 1}$, can be very easily estimated, in a maximum likelihood sense, with the following formula (units: nats per unit time):

$$T_{2 \to 1} = \frac{C_{11} C_{12} C_{2,d1} - C_{12}^2 C_{1,d1}}{C_{11}^2 C_{22} - C_{11} C_{12}^2},$$

where C_{ij} is the sample covariance between X_i and X_j, and $C_{i,dj}$ the sample covariance between X_i and $\bar{X}_j = \frac{X_{j,n+1-X_j}}{\Delta t}$ (Δt is the time step size). Also a statistical significance test can be performed (Liang, 2015); in the present study, the computed causality is at a 95% significance level. For more details, refer to (Liang, 2008, 2014, 2015, 2016).
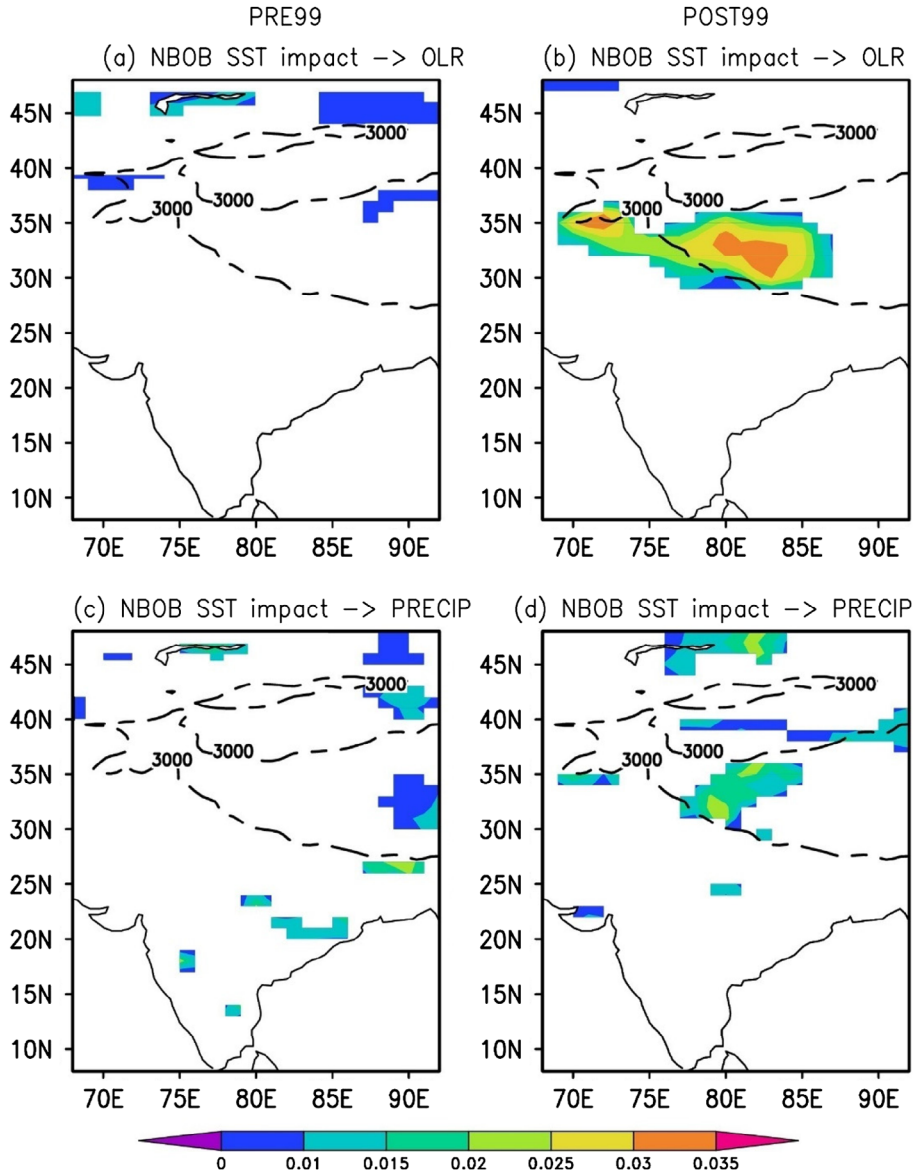
Fig. 5. (a) The causality (information flow) from the NBOB SST to OLR during PRE99. (b) Same as (a), but for POST99. (c) Same as (a) but for precipitation. (d) Same as (b) but for precipitation. The numbers are significant at a 95% level. The dashed line marks the 3000 m topographic contour. In the figures, the units are nats/day. Nat and bit are two common units for information and entropy, which has the form of logρ (ρ is the probability density function) followed by a mathematical expectation. If the logarithm uses a base 2, then the unit is *bit*; if it uses a base *e*, then the unit is *nat*.

The causality analysis result is plotted in Fig. 5. Interestingly, distinctly different impacts of the NBOB SST on the OLR and precipitation for the two different epochs are observed (Fig. 5). The results show that the NBOB SST has a large impact on the convection and precipitation over the western TP during POST99, while before 1999, it is by far insignificant. It is noteworthy to mention that the results obtained here are strictly unidirectional, i.e. the causalities from NBOB SST to OLR and precipitation, which cannot be obtained using the traditional correlation analysis. Besides, not only have we been able to determine the directions of causality, but also the magnitudes. From the figures the regions of significant causality from NBOB SST to PRECIP is within that from NBOB SST to OLR. This remarkable result from another aspect distinguishes the role of NBOB SST on the western TP during the two different climatic periods.

The TP is one of the major highly elevated land areas in the world and observed to have huge impacts on the surrounding countries. It is prone to abundant rainfall and flooding episodes during the peak summer monsoon, but the reason has
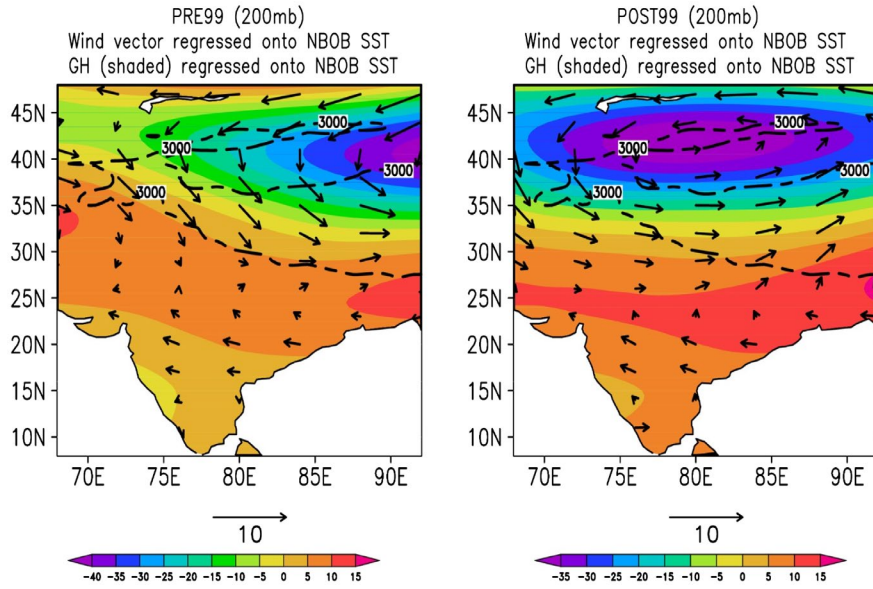
Fig. 6. Wind vector (arrow; units in m/s) and geopotential height (shaded; units in m) at 200mb regressed onto the JA NBOB SST for PRE99 (left panel) and POST99 (right panel). The regression coefficients are statistically significant at a 99% level. Shown are the regressed wind vectors and geopotential height on a 1°×1° latitude–longitude grid. The dashed line marks the 3000 m topographic contour.
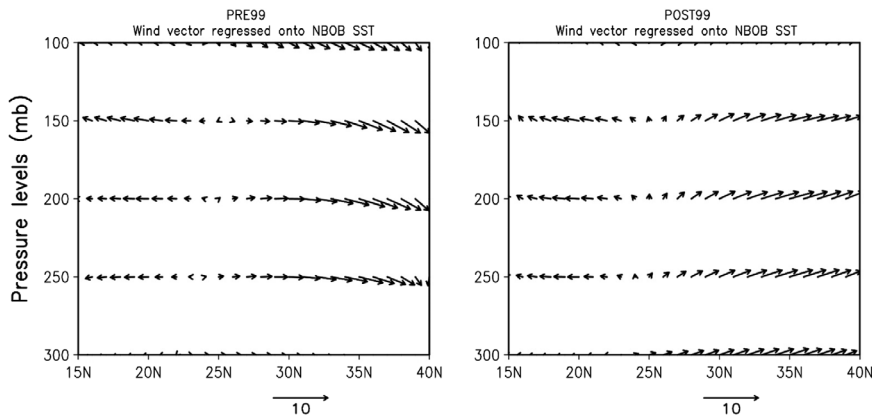

Fig. 7. The longitudinally averaged (75°E – 90°E) wind vector (arrow; units in m/s) and wind magnitude (shaded; units in m/s) at different pressure levels regressed onto the JA NBOB SST for PRE99 (left panel) and POST99 (right panel). The regression coefficients are statistically significant at a 99% level based on the student's test. Shown are regressed wind vectors on a 1°×1° latitude–longitude grid.

been poorly understood, despite the great scientific importance. These rainfalls on one hand have an agricultural importance, as the region's population depends greatly on monsoon rains, and on the other hand, lead to landslides, the most devastating hazards in the region. To see how the climate over the western TP may differ during the two epochs, the winds at 200mb level are regressed onto the NBOB SST. As shown in Fig. 6, during POST99, the NBOB SST seems to be concomitant with the western TP, with a noticeable circulation positioned over the Plateau, whereas during PRE99 the circulation is not over there (Fig. 6). Geopotential height analysis for the two periods also results in remarkable findings (Figs. 6a and b); shaded). Since

the vertical variation of winds is considered to be the basic element driving the convection over the region, we proceed to regress the vertical variations of winds averaged over 75°-90°E onto the NBOB SST. From Fig. 7, it is evident that the impact of NBOB SST is more noticeable during POST99 than during PRE99. During the POST99, the ascending winds (a sign of convection) are clearly seen at the upper vertical levels over the western TP, while during PRE99 no such phenomenon is observed (Fig. 7). The cause of the ascending winds can be understood through analysing the air temperature regressed onto the NBOB SST (Fig. 8). Interestingly, during POST99 (Fig. 8c and d), the NBOB SST is seen to induce a thermal contrast between
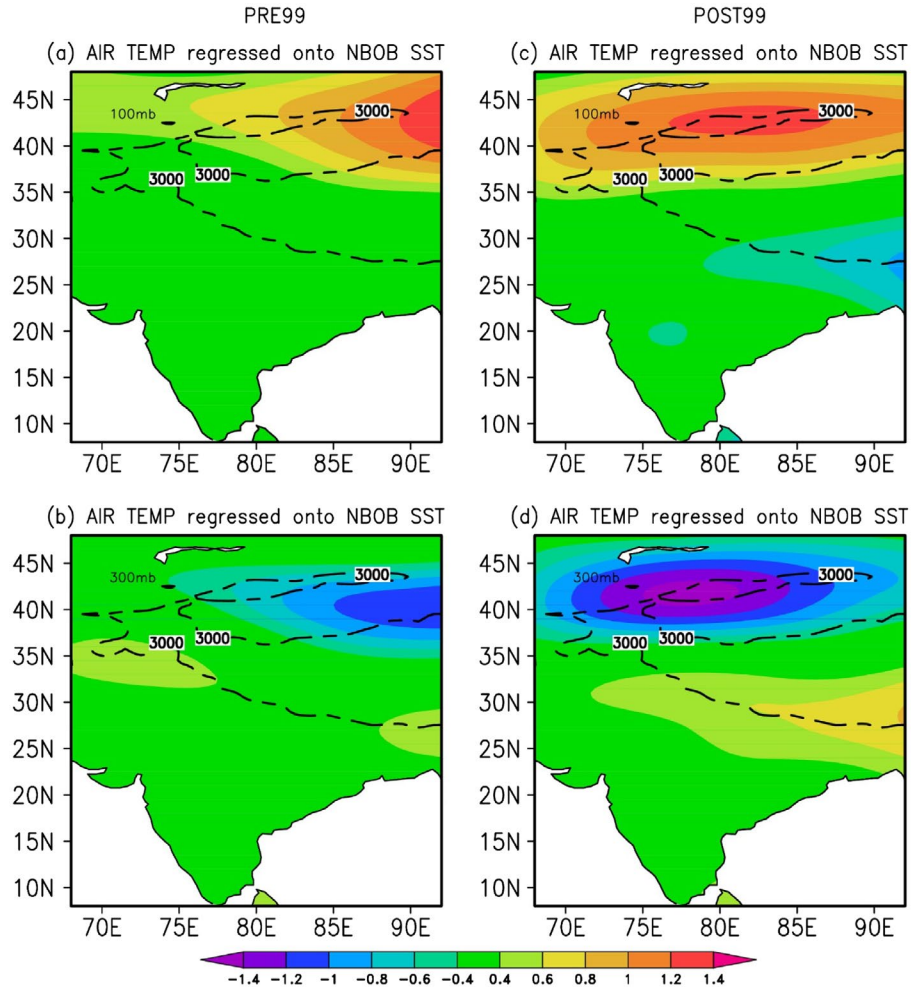
Fig. 8. (a) The air temperature (in K) at 100mb regressed onto the JA NBOB SST for PRE99. (b) Same as (a) but for 300mb. (c) Similar as (a) but for POST99. (d) Similar as (b) but for POST99. The regression coefficients are statistically significant at a 99% level. Shown is regressed air temperature on a 1° × 1° latitude–longitude grid. The dashed line marks the 3000 m topographic contour.

the 300mb and 100mb levels over the region 75°–90°E; that is to say, it seems to be responsible for the ascending winds in Fig. 7. This is in contrast to PRE99, when no such phenomenon is observed over the region. Based on these analyses, we can say that, since late 1990s, the relation of the NBOB SST with the western TP is being enhanced; this is because the NBOB SST induces a conspicuous circulation over the region.

4. Concluding remarks

We have analysed the daily mean NOAA SST data in the northern BOB during the July and August (the principal monsoon months in India) of 1988 to 2009. We found that the NBOB SST has distinctly different evolutionary patterns before and after 1999, which we refer to as PRE99 and POST99, respectively. A significant increase in NBOB SST was observed since late 1990s. Prior to 1999, the NBOB SST reveals a decreasing

trend, whereas after 1999 the trend is increasing. Same trend changes were observed for the outgoing long wave radiation and sensible heat flux. Further analysis shows that the NBOB SST facilitates the deep convection during POST99 and thereby impact the monsoonal convection over the surrounding regions. Remarkably, a large impact of NBOB SST on the convection and precipitation over the western TP during POST99 was revealed, whereas during PRE99 the impact was not much seen. During POST99, the NBOB SST seems to be concomitant with the western TP, with a conspicuous cyclonic circulation over the western TP, whereas during PRE99 the circulation is away from the Plateau; correspondingly, it occurs that the NBOB SST induces ascending winds between 300mb and 100mb levels during POST99.

We remark that the enhanced relationship of the NBOB SST with the western TP in the peak monsoon season of India in late 1990s may shed new insight into the various processes

associated the hydrology and geomorphology in the TP. They are of burgeoning scientific attention during the recent decade because of the occurrence of extreme weather events in the region during the season, which lead to severe flashfloods, landslides, property damages, injuries and even large number of fatalities (Liu et al., 2006).

Acknowledgments

Disclosure statement

No potential conflict of interest was reported by the authors.

Funding

References

Alam, M., Hossain, A. and Shafee, S. 2003. Frequency of Bay of Bengal cyclonic storms and depressions crossing different coastal zones. *Int. J. Climatol.* **23**, 1119–1125.

Anber, U., Wang, S. and Sobel, A. 2014. Response of atmospheric convection to vertical wind shear: cloud-system-resolving simulations with parameterized large-Scale circulation. Part I: specified radiative cooling. *J. Atmos. Sci.* **71**, 2976–2993. DOI:10.1175/JAS-D-13-0320.1.

Bruce, J. G. 1968. Comparison of near surface dynamic topography during the two monsoons in the western Indian Ocean. *Deep Sea Res.* **15**, 665–667.

Casey, K. S., Brandon, T. B., Cornillon, P. and Evans, R. 2010. The past, present and future of the AVHRR pathfinder SST program. In: *Oceanography from Space: Revisited* (eds. V. Barale, J. F. R. Gower and L. Alberotanza). Springer, Dordrecht, Netherlands, pp. 273–287. DOI:10.1007/978-90-481-8681-5_16.

Chen, B., Xu, X., Yang, S. and Zhang, W. 2012. On the origin and destination of atmospheric moisture and air mass over the Tibetan Plateau. *Theoret. Appl. Climatol.* **110**, 423–435.

Chung, P. H. and Li, T. 2013. Interdecadal relationship between the mean state and El Nino types. *J. Clim.* **26**(2), 361–379.

Dorji, T., Totland, O., Moe, S. R., Hopping, K. A. and Pan, J., and co-authors. 2013. Plant functional traits mediate reproductive phenology and success in response to experimental warming and snow addition in Tibet. *Global Change Biol.* **19**, 459–472.

Gadgil, S., Joseph, P. V. and Joshi, N. V. 1984. Ocean-atmosphere coupling over monsoon regions. *Nature* **312**, 141–143.

Gadgil, S., Rajeevan, M. and Nanjundiah, R. 2005. Monsoon prediction – Why yet another failure? *Curr. Sci.* **88**, 1389–1400.

Girishkumar, M. S. and Ravichandran, M. 2012. The influences of ENSO on tropical cyclone activity in the Bay of Bengal during October–December. *J. Geophys. Res.* **117**, C02033. DOI:10.1029/2011JC007417.

Girishkumar, M., Ravichandran, M. and Han, W. 2013. Observed intraseasonal thermocline variability in the Bay of Bengal. *J. Geophys. Res. Oceans* **118**, 3336–3349. DOI:10.1002/jgrc.20245.

Graham, N. E. and Barnett, T. P. 1987. Sea surface temperature, surface wind divergence and convection over the tropical oceans. *Science* **238**, 657–659.

Hacker, P., Firing, E. and Hummon, J. 1998. BOB currents during the northeast monsoon. *Geophys. Res. Lett.* **25**, 2769–2772.

Kalnay, E., Kanamitsu, M., Kistler, R., Collins, W. and Deaven, D., and co-authors. 1996. The NCEP/NCAR 40-year reanalysis project. *Bulletin of the American Meteorological Society* **77**, 437–472. DOI:10.1175/1520-0477(1996)077<0437:TNYRP>2.0.CO;2.

Kanamitsu, M., Ebisuzaki, W., Woollen, J., Yang, S. K. and Hnilo, J. J., and co-authors. 2002. NCEP-DOE AMIP-II Reanalysis (R-2). *Bull. Am. Meteorol. Soc.* **83**, 1631–1643.

Lau, K. M., Wu, H. T. and Bony, S. 1997. The role of large-scale atmospheric circulation in the relationship between tropical convection and sea surface temperature. *J. Clim.* **10**(3), 381–392.

Liang, X. S. 2008. Information flow within stochastic systems. *Phys. Rev. E* **78**, 031113.

Liang, X. S. 2014. Unraveling the cause-effect relation between time series. *Phys. Rev. E* **90**, 052150.

Liang, X. S. 2015. Normalizing the causality between time series. *Phys. Rev. E.* **92**, 022126.

Liang, X. S. 2016. Information flow and causality as rigorous notions *ab initio*. *Phys. Rev. E.* **94**, 052201.

Liu, X., Yin, Z. Y., Shao, X. and Qin, N. 2006. Temporal trends and variability of daily maximum and minimum, extreme temperature events, and growing season length over the eastern and central Tibetan Plateau during 1961–2003. *J. Geophys. Res.* **111**, D19109. DOI:10.1029/2005JD006915.

Ma, Y., Ma, W., Zhong, L., Hu, Z., Li, M., and co-authors. 2017, Monitoring and Modeling the Tibetan Plateau's climate system and its impact on East Asia. *Sci. Rep.* **7**, 44574; doi: 10.1038/srep44574.

McCreary, J. P., Kundu, P. K. and Molinari, R. L. 1993. A numerical investigation of dynamics, thermodynamics and mixed-layer processes in the Indian Ocean. *Progress in Oceanography* **21**, 181–244.

Molg, T., Maussion, F. and Scherer, D. 2014. Mid-latitude westerlies as a driver of glacier variability in monsoonal High Asia. *Nat. Clim. Change* **4**, 68–79.

Oliver, E. C. and Thompson, K. R. 2010. Madden-Julian Oscillation and sea level: local and remote forcing. *J Geophys Res* **115**, c01003. DOI:10.1029/2009JC005337.

Polanski, S., Fallah, B., Prasad, S. and Cubasch, U. 2013. Simulation of the Indian monsoon and its variability during the last millennium. *Clim Past Discuss* **9**(1), 703–740. DOI:10.5194/cpd-9-703-2013.

Raghavan, K. 1973. Break-monsoon over India. *Mon. Wea. Rev.* **101**, 33–43. DOI:10.1175/1520-0493(1973)101<0033:BOI>2.3.CO;2.

Rajeevan, M., Gadgil, S. and Bhate, J. J. 2010. Active and break spells of the Indian summer monsoon,. *Earth Syst. Sci.* **119**, 229–247. DOI:10.1007/s12040-010-0019-4.

Rao, S. A., Gopalakrishna, V. V., Shetye, S. R. and Yamagata, T. 2002. Why were cool SST anomalies absent in the BOB during the 1997 Indian Ocean Dipole Event? *Geophysical Research Letters* **29**, 1555. DOI:10.1029/2001GL014645.

Reynolds, R. W., Smith, T. M., Liu, C., Chelton, D. B., Casey, K. S., and co-authors. 2007. Daily high-resolution-blended analyses for sea surface temperature. *J. Climate* **20**, 5473–5496.

Roxy, M. and Tanimoto, Y. 2007. Role of SST over the Indian Ocean in influencing the intraseasonal variability of the Indian summer monsoon. *J. Met. Soc. Japan* **85**(3), 349–358.

Salahuddin, A., Isaac, R. H., Curtis, S. and Matsumoto, J. 2006. Teleconnections between the sea surface temperature in the Bay of Bengal and monsoon rainfall in Bangladesh. *Global Planet Change* **53**, 188–197. DOI:10.1016/j.gloplacha.2006.06.001.

Schott, F. A. and McCreary, J. P. 2001. The monsoon circulation of the Indian Ocean. *Prog Oceanogr* **51**, 1–123. DOI:10.1016/S0079-6611(01)00083-0.

Shankar, D., Vinayachandran, P. N. and Unnikrishnan, A. S. 2002. The monsoon currents in the north Indian Ocean. *Prog Oceanogr* **52**, 63–120.

Shenoi, S. S. C., Shankar, D. and Shetye, S. R. 2002. Differences in heat budgets of the near-surface Arabian Sea and BOB: implications for the summer monsoon. *J. Geophys. Res.* **107**, 1–14. DOI:10.1029/2000JC000679.

Singh, O. P., Ali Khan, T. M. and Rahman, M. S. 2001. Probable reasons for enhanced cyclogenesis in the Bay of Bengal during July-August of ENSO years, Global Planet. *Change.* **29**, 135–147.

Vaid, B. H. and Liang, X. S. 2015. Tropospheric temperature gradient and its relation to the South and East Asian precipitation variability. *Meteorol Atmos Phys* **127**(3), 579–585. DOI:10.1007/s00703-015-0385-1.

Webster, P. J. 1995. The annual cycle and the predictability of the tropical coupled ocean-atmosphere system. *Meteorol. and Atmos. Phys.* **56**, 33–55.

Wu, G. and Zhang, Y. 1998. Tibetan Plateau forcing and the timing of the monsoon onset over South Asia and the South China Sea. *Mon, Weather Rev.* **126**, 913–927.

Xiang, B., Wang, B. and Li, T. 2013. A new paradigm for the predominance of standing Central Pacific Warming after the late 1990s. *Clim. Dyn.* **41**(2), 327–340.

Xu, X., Lu, C., Shi, X. and Gao, S. 2008a. World water tower: An atmospheric perspective. *Geophys. Res. Lett.* **35**, L20815.

Xu, X. D., Shi, X. Y., Wang, Y. Q., Peng, S. Q. and Shi, X. H. 2008b. Data analysis and numerical simulation of moisture source and transport associated with summer precipitation in the Yangtze River Valley over China. *Meteorol Atmos Phys* **100**(1), 217–231. DOI:10.1007/s00703-008-0305-8.

Xue, Y., Hu, Z., Kumar, A., Banzon, V., Smith, T. M., and co-authors. 2013. Global Oceans] Sea surface temperatures [in "State of the Climate in 2012". *Bull Am Meteorol Soc (BAMS)* S47–S50.

Yang, K., Wu, H., Qin, J., Lin, C., Tang, W., and co-authors. 2014. Recent climate change over the Tibetan Plateau and their impacts on energy and water cycle, A review. *Glob. Planet. Change* **112**, 79–91.

Yao, T., Thompson, L., Yang, W., Yu, W., Gao, Y., and co-authors. 2012. Different glacier status with atmospheric circulations in Tibetan Plateau and surroundings. *Nat. Clim. Change* **2**, 663–667.

Yatagai, A., Kamiguchi, K., Arakawa, O., Hamada A., Yasutomi, N., and co-authors. 2012. APHRODITE: constructing a long-term daily gridded precipitation dataset for Asia based on a dense network of rain gauges. *Bull Am Meteorol Soc.* **24**, 1401–1415. DOI:10.1175/BAMS-D-11-00122.1.

Yuan, D. and Han, W. 2006. Roles of equatorial waves and western boundary reflection in the seasonal circulation of the equatorial Indian ocean. *J Phys Oceanogr.* **36**, 930–944.